Middle-East Journal of Scientific Research 18 (7): 983-990, 2013
ISSN 1990-9233

DOI: 10.5829/idosi.mejsr.2013.18.7.12237

The Mechanical and Electrical Characteristics of a 3C-SIC for Mems Capacitive Pressure Sensor Diaphragm

[1]Noraini Marsi, [1]Burhanuddin Yeop Majlis, [1]Azrul Azlan Hamzah, [1]Jumril Yunas and [2]Faisal Mohd-Yasin

[1]Institute of Microengineering and Nanoelectronics (IMEN),
Universiti Kebangsaan Malaysia, Malaysia
[2]Queensland Micro- and Nanotechnology Centre (QMNC),
Griffith University, 4111 Brisbane, Australia

Abstract: Silicon carbide (3C-SiC) is promising materials due to many desirable characteristics that make it an excellent material for the fabrication MEMS capacitive pressure sensor operate in harsh environment. The main novelty of this work involves the use of (3C-SiC) thin film as the flexible plate, which is anisotropically etch with fixed plate being bonded by a silicon substrate. The MEMS capacitive pressure sensor is simulated using COMSOL ver 4.3 for mechanical and electrical verification. This work compares the design of a diaphragm-based MEMS capacitive pressure sensor employing 3C-SiC and Si thin films operating at extreme temperature which is 1000°C. Both materials are designed with the same area, but with different thickness of diaphragm which is 1.0 μm, 1.6 μm and 2.2 μm. In this paper, we study the effects of pressure across the temperature, capacitance performances and the maximum Von Mises Stress simulation in the center of diaphragm element. We also compare the mechanical and electrical characteristics between two materials. The 3C-SiC thin film is far superior to Si thin film mechanically to withstand an applied pressure, temperature that affect the Von Mises Stress up to 148.32 MPa, the maximum output capacitance of 1.93 pF is achieved with less total energy of 5.87 x 10^{-13} J, thus having a 50 % saving as compared to Si.

Key words: Silicon carbide · COMSOL ver 4.3 · MEMS · Von Mises Stress · Harsh environment

INTRODUCTION

There has been a tremendous development in field of robust micro-mechanical-system (MEMS) for harsh environment such as MEMS pressure sensor have been widely used in gas turbine engine, automobiles, airplanes, submarines and biomedical devices [1]. MEMS pressure sensor based silicon (Si) sensors are not suitable for harsh environment applications because of the limitation its mechanical and electrical properties that can degrade below temperature of 500°C [2]. It suggests that these challenges can be overcome through developing alternative materials to replace Si for MEMS application. Silicon carbide (3C-SiC) is promising materials due to many desirable characteristics that make it an excellent material for the fabrication MEMS capacitive pressure sensor operate in harsh environment [3].

The material properties of 3C-SiC make it an effective material are highly wear resistant with good mechanical and electrical properties including high temperature strength, high hardness and excellent thermal shock resistance applications. 3C-SiC also has an excellent electrical characteristic such as wide band-gap (2.3 eV), high-saturated drift velocity (2.5 x 10^{7} cms^{-1}), high breakdown field (1.8 x 10^{17} cm^{-3}), higher thermal conductivity (5 W/cm-K) and electrically robust that have been adequately applied in a high temperature, harsh environment and high power density for MEMS

Corresponding Author: Noraini Marsi, Institute of Microengineering and Nanoelectronics (IMEN), Universiti Kebangsaan Malaysia, 43600 Bangi, Selangor, Malaysia.
Tel: +603 8911 8020, Fax: +60389250439.

application [4]. Although, the 3C-SiC is a mechanically superior material compared to silicon that can remains constant up to temperature above 1400 °C with relatively high Young's modulus of 450 GPa, higher yield strength (21 GPa), higher density (3.2 x 10^{-15} kg/µm^{-3}), Poisson's ration of 0.22 and mechanically the MEMS device that can operate effectively at extreme temperature environment [5].

In this paper, specifically compares the mechanical and electrical performance of the movable diaphragm utilizing both materials 3C-SiC and Si at different thicknesses of diaphragm which is 1.0 µm, 1.6 µm and 2.2 µm under the same conditions of pressure and temperature. The design and modeling of MEMS capacitive pressure sensor is simulated an analyzed by using COMSOL Multiphysics software ver. 4.3 that have a graphical and interactive simulation. In this MEMS device, we present results showing the effect of diaphragm center deflection, capacitance values for the effects of mechanical deflection; Von Mises Stresses distribution into loaded diaphragm and total electric energy which deflect in response to applied pressure.

MATERIALS AND METHODS

Modeling of MEMS Capacitive Pressure Sensor Design: In order to the design and optimization of such integrated MEMS devices, COMSOL Multiphysic software ver. 4.3 is used to design the 3D MEMS capacitive pressure sensor as shown in Fig. 1. A detailed 2D cross section of the functional part of the MEMS capacitive pressure sensor is shown in Fig. 2. A thin diaphragm is held at a fixed potential of 1 Volt. The MEMS capacitive pressure sensor made up of three layers. The diaphragm is separated from the substrate by a cavity with the thickness of 2.2 µm in the atmospheric pressure inside as a reference pressure. The insulator is to prevent a connection between the diaphragm and the silicon substrate.

When external pressures are applied, the diaphragm deflects towards the substrate. The distance between the diaphragm and the substrates decreases, exhibiting changes dramatically increasing its capacitance. Once the diaphragm touches the substrate due to the change of touched area, the capacitance will increase nearly linearly with increasing pressure [6]. Different parameters such as diaphragm thickness and square shape of MEMS capacitive pressure sensor as well as dielectric layer

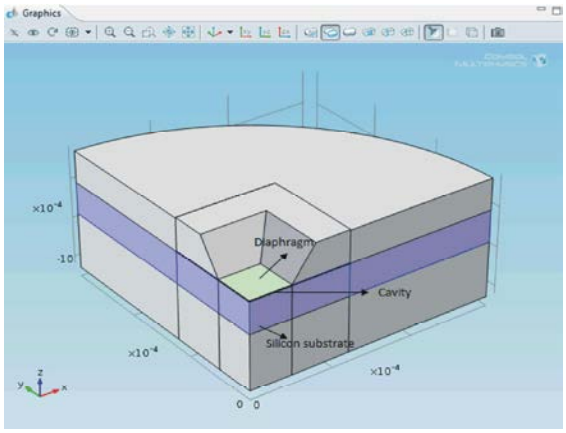

Fig. 1: Modeling of 3D MEMS capacitive pressure sensor.

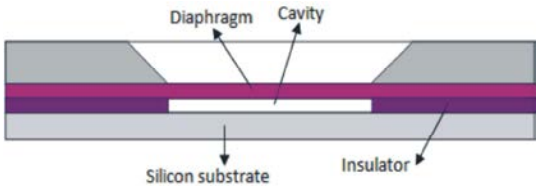

Fig. 2: Cross section through the MEMS capacitive pressure sensor.

MEMS capacitive pressure sensors with various specifications such as linear range, sensitivity and capacitances values.

Simulation:

Deflection Performance for 3C-SiC and Si: In order to analyze the deflection performance, both 3C-SiC and Si materials of MEMS capacitive pressure sensor design were simulated. For both materials, the diaphragm thickness is differential of 1.0 µm, 1.6 µm and 2.2 µm and the gap cavity between the diaphragm and substrate were fixed at 2.2 µm. The diaphragm is square shape with width and length of 200 µm. Model builder solver was analyzing the deflection performance. The diaphragm centre deflection $w(x$ for square shape of MEMS capacitive pressure sensor can be defined as [7]:

$$W_{\max} = 0.01512\left(1-v^2\right)\frac{p}{E} \quad (1)$$

Note that P is pressure on diaphragm, E is Young's modulus, h is thickness of plate, L is the length, v is Poisson's ratio of the diaphragm material and w is vertical deflection of diaphragm.

Capacitance Performance for 3C-SiC and Si: In order to analyze the capacitance performance of MEMS capacitive pressure sensor design, Model builder solver was used to analyze the capacitance performance. The capacitance equation can be defined as [8]:

$$C = \frac{\varepsilon_r \varepsilon_0 A}{d} \tag{2}$$

Where C is the capacitance between the two electrodes, ε_r is the permittivity of the dielectric medium used between the two electrodes, ε_0 is the permittivity for air (8.854×10^{-14} F/cm) and d is the distance or separation between two electrodes. To analyze the capacitance performance for both materials, the differential thicknesses of the diaphragm of 1.0 µm, 1.6 µm and 2.2 µm are varied and the resulting capacitances between two materials were compared.

Von Mises Stress Performance: When 3C-SiC and Si diaphragm is subject to increasing loads it eventually fails. It is comparatively easy to determine the point of failure of a diaphragm by applied pressure. The Von Mises Stresses on both materials indentifies by their mechanical strength. The maximum Von Mises Stress criterion is based on the Von Mises-Hencky theory, also known as the shear-energy theory or maximum distortion energy theory [9].

Fig.3 shows the 2D state of stress with the independent stress components of σ_x and σ_y. A third stress component σ_3 can exist on the z-axis. In term of the principle stresses σ_x, σ_y and σ_z, the Von Mises Stress is expressed as to relate failure to this state of status, three important indicators are derived; principle stress, maximum shear stress and Von Mises Stress [10].

Principle Stresses:

$$\sigma_1, \sigma_2 = \frac{\sigma_x + \sigma_y}{2} \pm \sqrt{\left(\frac{\sigma_x - \sigma_y}{2}\right) + \tau_{xy}^2} \tag{3}$$

$$\sigma_3 = 0 \tag{4}$$

Maximum shear stress:

$$\tau_{\max,1,2} = \frac{\sigma_1 - \sigma_2}{2} \tag{5}$$

$$\tau_{\max,1,3} = \frac{\sigma_1 - \sigma_3}{2} \tag{6}$$

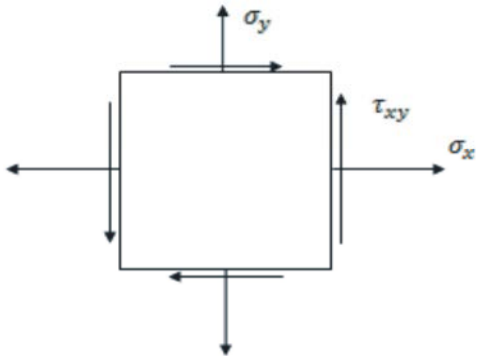

Fig. 3: 2D stress components

$$\tau_{\max,2,3} = \frac{\sigma_2 - \sigma_3}{2} \tag{7}$$

The Von Mises Stress:

$$\sigma_v = \sqrt{\frac{(\sigma_1 - \sigma_2)^2 + (\sigma_2 - \sigma_3)^2 + (\sigma_1 - \sigma_3)^2}{2}} \tag{8}$$

When $\sigma_3 = 0$, the Von Mises Stress is:

$$\sigma_v = \sqrt{\sigma_1^2 + \sigma_2^2 - \sigma_1 \sigma_2} \tag{9}$$

When only σ_x and τ_{xy} are present (as in combined torsion and bending/axial stress), there is no need to calculate the principle stress, the Von Mises Stress is:

$$\sigma_v = \sqrt{\sigma_x^2 + 3\tau_{xy}^2} \tag{10}$$

Total Electric Energy Performance: A charged between electrode diaphragm and substrate experiences a force from pressure when it is in a region where an electric field exists. From the definition of the electric field, this force is given by [11]:

$$\vec{F} = q\vec{E} \tag{11}$$

Where F the force is exerted on the electrode diaphragm, q is the charge of the particle between electrodes and E is the electric field. When an electron (q=-e) is in an electric field, the electron experiences a force in the direction opposite of the electric field by applying a potential

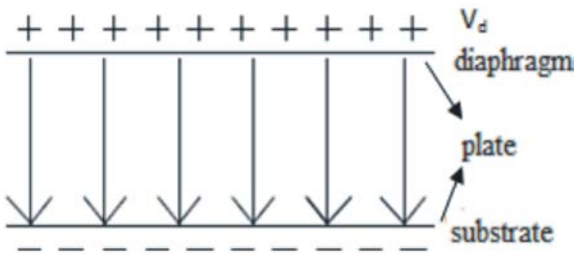

Fig. 4: The electric field in MEMS pressure sensor

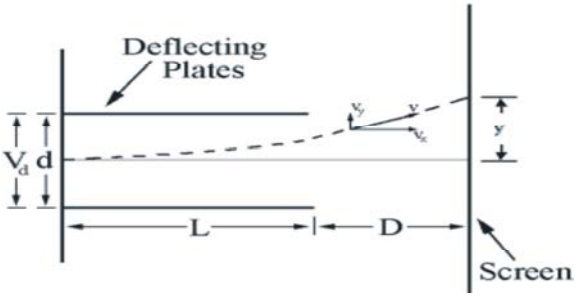

Fig. 5: Effect deflection plates with electrical energy

difference V_{acc} between two electrodes. m is the mass of the electron. Electrons enter deflecting plates having a velocity, v_x given by [12]:

$$v_x = \sqrt{\frac{2eV_{acc}}{m}} \tag{12}$$

Once the electrons leave to another electrode, they have create a uniform electric field in the region between the deflecting plates by applying a voltage, V_d=*1Volt*, across the plates, as seen in Fig.4.

The strength of the electric field is given by [13]:

$$E_y^{deflect} = -\frac{dV}{dy} = -\frac{V_d}{d} \tag{13}$$

The average field by replacing the derivative with the voltage difference divided by d, the distance between the plates. However, for large deflection, diaphragm plates are applied by different uniform pressure, so that the average field and the local field are quite close in value. The electric field will exert a force on the electron, opposite the direction of the arrow in Fig.4, causing the trajectory of the electron on be altered, as seen in Fig. 5. A negatively charged electron is deflected in an electric field. It is repelled from the negative plate and attracted towards the positive plate.

Using Newton's second law and the kinematic equations, the distance the electron is deflected is given by [14]:

$$y = \frac{eE_y^{deflect}L}{mv_x^2}\left(D + \frac{L}{2}\right)$$

Where L is the length of the plates, d is their separation and D is the distance from the end of the plates to the viewing screen.

RESULTS AND DISCUSSION

Deflection Versus Pressure of the Diaphragm: Fig. 6 and Fig.7 show the deflection of the diaphragm when a pressure is applied on the surface. Based on the results, shows that the deflection on 1.6 µm and 2.2 µm thickness of diaphragm in a uniform potential when increasing pressure is applied on the surface of the diaphragm not in contact between the plates while for 1.0 µm, the deflection is non-uniform. This is indicates that the 3C-SiC material with a thicker diaphragm exhibited higher efficiency. The diaphragm of uniform deflection can withstand substantially higher pressure up to 120 kPa with deflection of 0.51 µm.

If a pressure has to be designed that shows a linear characteristic line, the characteristic line gets more linear by increasing the thickness of the diaphragm, which enlarges the equation (1). In Fig.8, the pressure increase is shown as a function of the deflection for different thickness of a diaphragm. As expected, the pressure increase is more linear function of the deflection for thicker diaphragm. It is an option to design a thicker diaphragm, if a linear interrelationship between pressure increase and deflection desired.

Capacitance with Pressure and Operating Temperature: Fig. 9 shows the effects of capacitance with operating temperature both materials 3C-SiC and Si using COMSOL ver.4.3. In MEMS capacitive pressure sensor, the diaphragm deflection modulates capacitance with respect to the substrate. Fig. 10 shows the increasing capacitance dependence on increasing pressure. The 3C-SiC exhibits a significant linear of capacitance versus increasing pressure up to 100 kPa while Si materials inherently non-linear characteristic has been introduced due to high pressure, stress and strain [15].

The diaphragm based 3C-SiC materials achieved large changes in capacitance with comparative performance of linear at high pressure of 100 kPa with the maximum

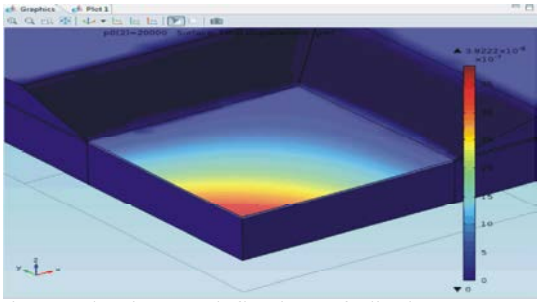

Fig. 6: The image deflection of diaphragm COMSOL software

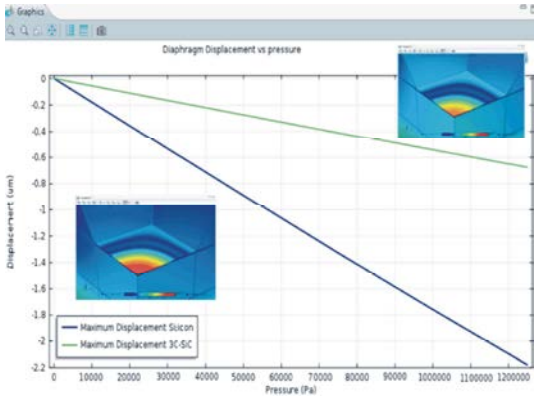

Fig. 7: Plot of deflection vs. pressure in COMSOL software

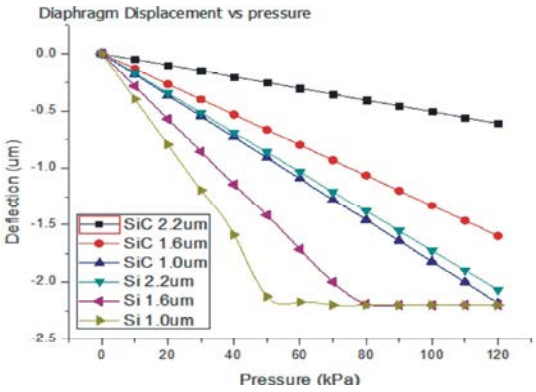

Fig. 8: Comparison of deflection vs. pressure for 3C-SiC and Si with differential thicknesses of diaphragm

capacitance of 1.93 pF compared Si of 1.22 pF. It is demonstrated that 3C-SiC has excellent materials incredibly high pressure. In contrasts, diaphragm based Si materials shows the capacitance decrease linearly with pressure until 80 kPa, however at 80 kPa, shows non-linearly relation between capacitance and pressure due to the material properties of Si does not endure high pressure that possibility effects the diaphragm were damaged very easily [16].

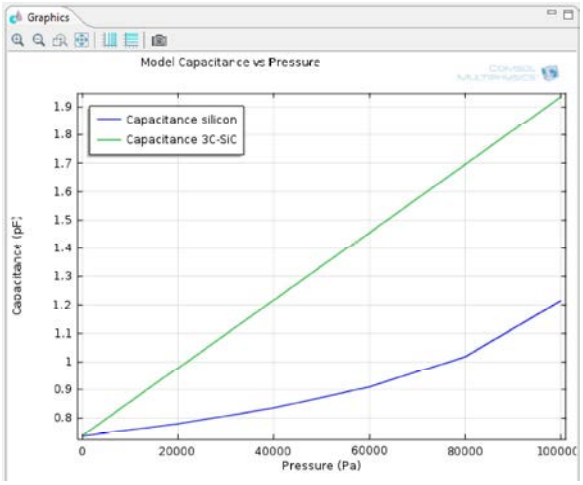

Fig. 9: Plot of capacitance vs. pressure in COMSOL

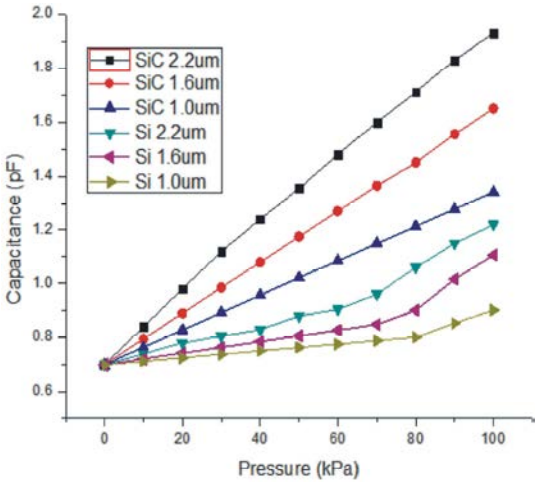

Fig. 10: Comparison of capacitance vs. pressure for 3C-SiC and Si with differential thicknesses of diaphragm

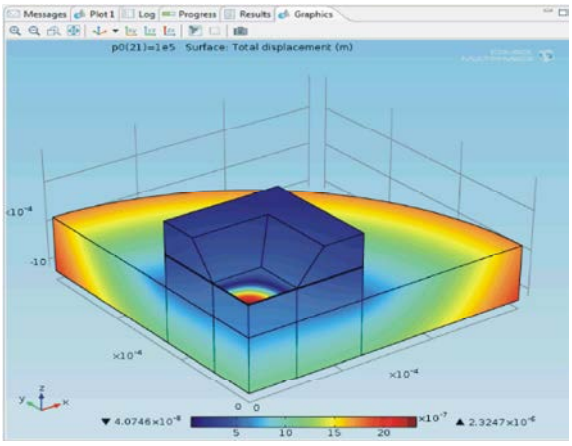

Fig. 11: The effects capacitance of diaphragm when pressure and temperature are applied

Fig. 11 shows the effects of 3D MEMS capacitive pressure sensor caused by applied pressure and temperature. Fig. 12 and Fig.13 shows the linear capacitance express dependence on operating temperature for 3C-SiC materials. The diaphragm based 3C-SiC materials exhibits large changes in capacitance at high temperature of 1000 °C with the maximum capacitance of 0.71 pF compared Si of 0.65 pF due to its relatively superior thermal and electrical properties. It is revealed 3C-SiC is able to function in extreme temperature, high power conditions will enable producing high performance enhancement to a wide variety of system and applications [17].

In contrasts, diaphragm based Si materials shows the capacitance decrease non-linear with operating temperature due to the limitation material properties of Si not be able to sustain at extreme temperature because of the dielectric losses caused by changing field strength limited and the mechanical properties of elastic modulus decreases with temperature, then describe that silicon are not suitable materials to be applied at extreme temperature applications [18].

Maximum von Mises Stress VS. Pressure and Temperature: Fig. 14 shows the Von Mises Stress distribution of the MEMS capacitive pressure sensor diaphragm. In Fig. 15 shows the Von Mises Stress plot of the results corresponding to pressure and operating temperature. The results show that the largest effect strain and stress appear at the diaphragm with the bigger thickness. For 3C-SiC, the highest Von Mises Stress is in the higher pressure is 100 kPa and temperature of 1000 °C with the value of 148.32 MPa compared to 125.48 MPa for Si with the same thickness of 2.2 μm. It is demonstrated the linear analysis indicates a uniform state of stress is proportional to the strain as referred to equation (8) function as well as high sensitivity for a pressure sensor equipped with such as diaphragm [19]. It is revealed that this material is good for resisting of high pressure and extreme temperatures.

For Si materials, the results present more realistic nonlinear responses to pressure and operating temperature stated that unconditional stability of the materials with respect to strain increments. It is possible that the high stresses monitored at these stress concentration areas due to thermal stresses caused by thermal expansion and contraction of the materials produced by thermal gradient [20-23]. The major thermal stress induced can cause failure of diaphragm materials effects the non-linear behavior.

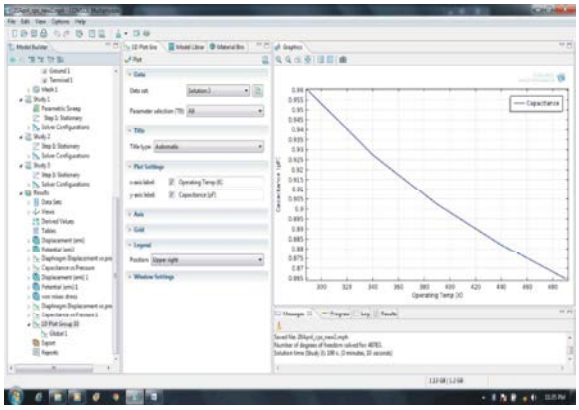

Fig. 12.: Plot of capacitance vs. operating temperature in COMSOL

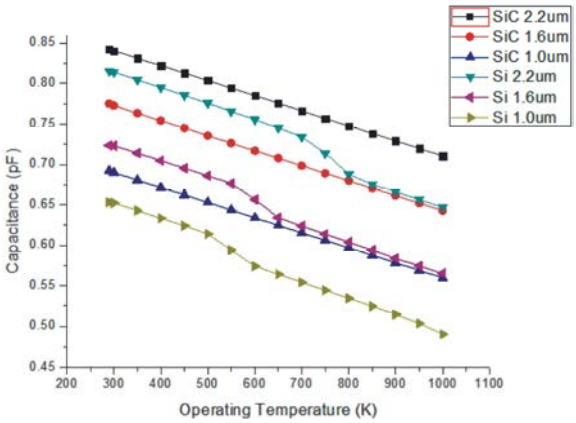

Fig. 13: Comparison of capacitance vs. operating temperature for 3C-SiC and Si with differential thickness of diaphragm

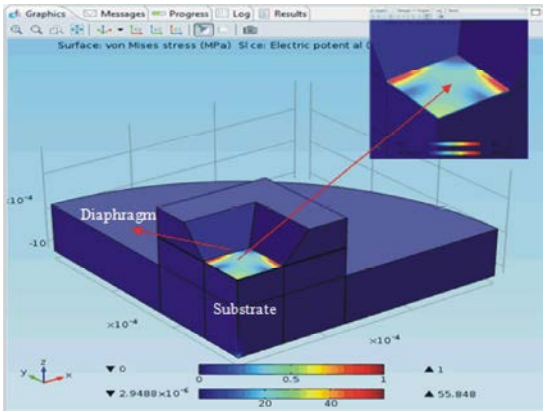

Fig. 14: The effects Von Mises Stress of diaphragm when pressure and temperature are applied

Total Electric Energy Performance with Applied Pressure: Fig. 16 shows the results of total electric energy versus pressure simulated in COMSOL software.

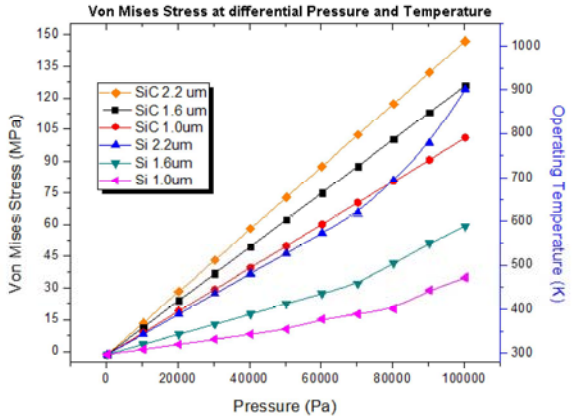

Fig. 15: Comparison of Von Mises Stress vs. pressure and temperature for 3C-SiC and Si with differential thickness of diaphragm

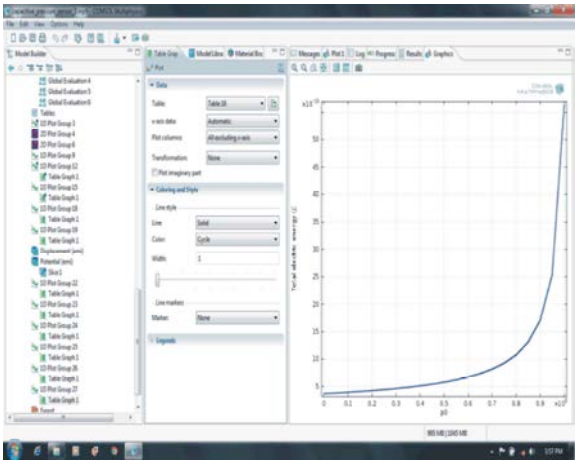

Fig. 16: Total electric energy results based COMSOL ver. 4.3 software

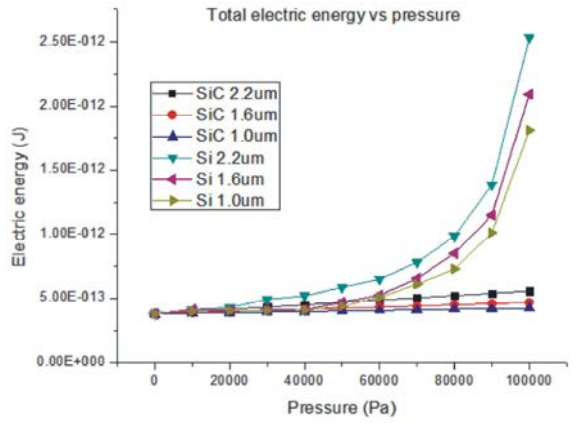

Fig. 17: Comparison of total electric energy vs. pressure for 3C-SiC and Si with differential thickness of diaphragm

The expression of total electric energy is defined by equation (11) for the center deflections due to electrical biasing field between two electrodes responding to pressure that are applied on the surface of diaphragm with the input voltage remaining 1 Volt.

Fig. 17 shows the effect of comparison total electrical versus pressure both materials 3C-SiC and Si. The electric energy of MEMS capacitive pressure sensor shows the increasing electric energy with increasing the pressure. However, for 3C-SiC material shows the lowest electric energy with electric energy less than 5.87 x 10^{-13} J compared Si of 2.53 x 10^{-12} J, thus having more than 50 % saving as compared to Si.

CONCLUSION

In conclusion, the MEMS capacitive pressure sensor based 3C-SiC diaphragm has been proven to be most suitable material to be applied at extreme temperature and high pressure. The 3C-SiC materials demonstrated the capacitance increase linearly with increasing of temperatures with maximum capacitance of 1.93 pF compared Si of 1.22 pF due to the fact that 3C-SiC thin film maintain its structural integrity of high Young's modulus and thermal conductivity that can withstand operate at extreme temperatures. In term of the maximum Von Mises Stress that is induced on the centre of the diaphragm, 3C-SiC thin films is performed better than its Si counterparts in the maximum Von Mises Stress of 148.32 Mpa at 1000 °C. In terms of electrical performance for 3C-SiC based sensor, the maximum output capacitance of 1.93 pF is achieved with less total electrical energy of 5.87 x 10-13 J, thus having a more than 50 % saving as compared to Si.

ACKNOWLEDGEMENTS

The authors would like to thank the Institute Microengineering and Nanoelectronic (IMEN) of Universiti Kebangsaan Malaysia (UKM), Science-fund MOSTI for supporting this project under grant 03-01-02-SF0849 and Queensland Micro- and Nanotechnology Centre (QMNC) of Griffith University for providing the resources and facilities in part at the Queensland node of the Australian National Fabrication Facility, a company established under the National Collaborative Research Infrastructure Strategy to provide nano and micro-fabrication facilities for Australia's researchers.

REFERENCES

1. Zhao, Q. and X. Xiong, 2010. MEMS Pressure Sensor for High-temperature Application. In the proceedings of the 2010 ASEE. The American Society for Engineering Education Northeast Section Conference, Boston.
2. Azevedo, R.G., J. Zhang and D.R. Myers, 2007. Silicon Carbide Coated MEMS Strain Sensor for Harsh Environment Applications. In the proceeding of the Micro electro Mechanical System, IEEE 20th International Conference, pp: 643-646.
3. Mehregany, M., C.A. Zorman, N. Rajan and C.H. Wu, 1998. Silicon Carbide MEMS for Harsh Environments. Journal of the IEEE, 86(8): 1594-1609.
4. Wijesundara, M.B.J. and R.G. Azevedo, 2011. Silicon Carbide Microsystems for Harsh Environments MEMS Reference Shelf, 22: 1-32.
5. Marsi, N., B.Y. Majlis, A.A. Hamzah and F. Mohd-Yasin, 2012. Comparison of Mechanical Deflection and Maximum Stress of 3C-SiC and Si-based Pressure Sensor Diaphragms for Extreme Environment. In the proceedings of the Semiconductor Electronics, ICSE, pp: 186-190.
6. Jiangang, D., J. Young, C.A. Zorman and W.H. Ko, 2003. Single Crystal SiC Capacitive Pressure Sensor at 400 °C. Electron Devices Meeting IEDM'03 Technical Digest, IEEE International, pp: 1-4.
7. Khakpour, R., S. Mansouri and A. Bahadorimehr, 2010. Analytical Comparison for Square, Rectangular and Circular Diaphragm in MEMS Applications. Journal of Electronic Devices, Systems and Applications, pp: 297-299.
8. Damghanian, M., 2009. Design and Fabrication of a MEMS Tactile Pressure Sensor Array for Fingerprint Imaging, in Universiti Kebangsaan Malaysia, Bangi, Malaysia.
9. Kurowski, P.M., 2012. Engineering Analysis with Solidworks Simulation. Schroff Development Corporation, pp: 22-25.
10. Tai-Ran, H., 2008. MEMS and Microsystems: Design, Manufacture and Nanoscale Engineering. John Wiley and Sons, pp: 175-180.
11. Zonnevylle, A.C., T. Verduin, C.W. Hagen and P. Kruit, 2013. Deflection Properties of An Electrostatic Electron Lens with a Shifted Electrode. Journal of Vacuum Science and Technology B, 31(6): 111-117.
12. Xiao, H., 2012. Dynamic Defocusing in Streak Tubes. Thesis of Laboratory for Laser Energetic, University of Rochester.
13. Zhang, Z., L. Li, X. Xie and D. Xiao, 2013. Optimization Design and Research Character of the Passive Electric Field Sensor. Sensors Journal, IEEE, Issue, pp: 99.
14. Experiments with an electron beam at http://visual.physics.tamu.edu/vp208/LabManual/Lab_3.pdf, retrieved on 30 October 2013
15. Hong-Yu, M., H. Qing-An, Q. Ming and L.Tingting, 2009. A Micromachined Silicon Capacitive Temperature Sensor for Radiosonde Applications. Sensor IEEE, pp: 1693-1696.
16. Medler, A.E., 1998. A Thin Monocrystalline Diaphragm Pressure Sensor Using Silicon-on-insulator Technology. Thesis Degree of Doctor of Philosophy, School of Engineering Systems, Middlesex University.
17. Marsi, N., B.Y. Majlis, F. Mohd-Yasin and A.A. Hamzah, 2013. The Capacitance and Temperature Effects of the SiC- and Si- based Mems Pressure Sensor. Journal of Physics Conference Series, 431: 1-9.
18. Gomes, J. and H.R. Shea, 2011. Displacement Damage Effects in Silicon MEMS at High Proton Doses. American Institute of Physics, pp: 7928.
19. Benmeddour, A. and S. Meziani, 2009. Numerical Study of Thermal Stress During Different Stages of Silicon Czochralski Crystal Growth, 12: 575-584.
20. Zang, M., D.L. Polla, S.M. Zurn and T. Cui, 1999. Stress and Deformation of Pzt Thin Film on Silicon Wafer due to Thermal Expansion. Materials Research Society Proceedings, pp: 574.
21. Sibghatullah Nasir, 2013. Microfinance in India: Contemporary Issues and Challenges, Middle-East Journal of Scientific Research, 15(2): 191-199.
22. Mueen Uddin, Asadullah Shah, Raed Alsaqour and Jamshed Memon, 2013. Measuring Efficiency of Tier Level Data Centers to Implement Green Energy Efficient Data Centers, Middle-East Journal of Scientific Research, 15(2): 200-207.
23. Hossein Berenjeian Tabrizi, Ali Abbasi and Hajar Jahadian Sarvestani, 2013. Comparing the Static and Dynamic Balances and Their Relationship with the Anthropometrical Characteristics in the Athletes of Selected Sports, Middle-East Journal of Scientific Research, 15(2): 216-221.